8540–8550 *Nucleic Acids Research, 2015, Vol. 43, No. 17* *Published online 6 August 2015*
doi: 10.1093/nar/gkv801

The FMRP/*GRK4* mRNA interaction uncovers a new mode of binding of the Fragile X mental retardation protein in cerebellum

Thomas Maurin[1,2,3,†], Mireille Melko[1,2,3,†], Sabiha Abekhoukh[1,2,3], Olfa Khalfallah[1,2,3], Laetitia Davidovic[1,2,3], Marielle Jarjat[1,2,3], Simona D'Antoni[4], Maria Vincenza Catania[4,5], Hervé Moine[6], Elias Bechara[1,2,3] and Barbara Bardoni[1,2,3,*]

[1]CNRS UMR 7275, Institute of Molecular and Cellular Pharmacology, 06560 Valbonne Sophia-Antipolis, France, [2]University of Nice Sophia-Antipolis, 06103 Nice, FRANCE, [3]CNRS LIA 'Neogenex', 06560 Valbonne Sophia-Antipolis, France, [4]Institute of Neurological Sciences, The National Research Council of Italy, 95126 Catania, Italy, [5]IRCCS Oasi Maria SS, 94018 Troina (EN), Italy and [6]IGBMC (Institut de Génétique et de Biologie Moléculaire et Cellulaire), CNRS, UMR7104, Inserm U596, Collège de France, Strasbourg University, 67400 Illkirch-Graffenstaden, France

Received January 15, 2015; Revised July 26, 2015; Accepted July 28, 2015

ABSTRACT

Fragile X syndrome (FXS), the most common form of inherited intellectual disability, is caused by the silencing of the *FMR1* gene encoding an RNA-binding protein (FMRP) mainly involved in translational control. We characterized the interaction between FMRP and the mRNA of *GRK4*, a member of the guanine nucleotide-binding protein (G protein)-coupled receptor kinase super-family, both *in vitro* and *in vivo*. While the mRNA level of *GRK4* is unchanged in the absence or in the presence of FMRP in different regions of the brain, GRK4 protein level is increased in *Fmr1*-null cerebellum, suggesting that FMRP negatively modulates the expression of GRK4 at the translational level in this brain region. The C-terminal region of FMRP interacts with a domain of *GRK4* mRNA, that we called G4RIF, that is folded in four stem loops. The SL1 stem loop of G4RIF is protected by FMRP and is part of the S1/S2 subdomain that directs translation repression of a reporter mRNA by FMRP. These data confirm the role of the G4RIF/FMRP complex in translational regulation. Considering the role of GRK4 in GABAB receptors desensitization, our results suggest that an increased GRK4 levels in FXS might contribute to cerebellum-dependent phenotypes through a deregulated desensitization of GABAB receptors.

INTRODUCTION

Fragile X syndrome (FXS) is the first cause of inherited intellectual disability (ID), affecting 1:4000 males and 1:7000 females and is characterized by moderate to severe ID, hyperactive behavior, autism, attention deficit, seizures and sleep disorders (1). The cause of FXS is the silencing of the *FMR1* gene encoding FMRP, a protein localized in various sub-cellular compartments (1). Indeed, FMRP is endowed with several RNA-binding domains (1,2) and is involved in different steps of RNA metabolism, namely RNA export from nucleus to cytoplasm, translational regulation and axonal/dendritic transport (1,3–4). To date, most laboratories have focused their study on the function of FMRP in translational control. Indeed, FMRP was shown to be mainly associated with translating polyribosomes (80–90%), suggesting that its main function is linked to translational regulation acting both as a repressor and as an enhancer of translation (4–8). A remarkable effort has been made during the last years to define a large set of mRNAs target of FMRP, but the vast majority of the candidates awaits further molecular characterization and the functional significance of these interactions need to be precisely defined (4). The analyses of FMRP target mRNAs also resulted in the identification of some motifs/structures mediating their interaction with FMRP and validating the implication of the FMRP/RNA complex in translational regula-

*To whom correspondence should be addressed. Tel: +33 4 93 95 77 66; Fax: +33 4 93 95 77 08; Email: bardoni@ipmc.cnrs.fr
†These authors contributed equally to the paper as first authors.
Present addresses:
Mireille Melko, Department of Molecular Biology and Genetics—Genome expression, stability and technology, AAHRUS University, Denmark.
Elias Bechara, CRG-Centre for Genomic Regulation, Barcelona, Spain.

tion, but not in transport (4,9–10). Indeed, G-quadruplex, kissing complex and ACUK/WGGA sequences have been involved in translational repression mediated by FMRP. Conversely, SoSLIP, a structure organized in three stem loops separated by short sequences, is an activator of translation '*per se*' and its activity is enhanced when bound by FMRP (4). Interestingly, according to a recent *in silico* prediction, several ACUK/WGGA sequences can be folded in G-quadruplex forming structures when present in some FMRP target mRNAs (11).

We characterized the interaction between FMRP and the mRNA of *GRK4*, a member of the guanine nucleotide-binding protein (G protein)-coupled receptor kinase superfamily, both *in vitro* and *in vivo*. FMRP negatively modulates the expression of GRK4 at the translational level by binding an RNA structure that was never previously described as target of FMRP. It has been shown that, in cerebellar granule cells, GRK4 interacts directly with the metabotropic $GABA_B$ receptor (GBR), promoting its desensitization (12). Cerebellum GBRs signaling has a pivotal role in motor learning and coordination (13). With this premise, the elevated level of GRK4 in *Fmr1*-null cerebellum could determine an increased desensitization of GBRs specifically in this brain region and contribute to deficits of motor learning and movement coordination that are cerebellum-dependent phenotypes of FXS (14).

MATERIALS AND METHODS

Reverse transcription (RT)-PCR and quantitative real-time PCR

Total RNAs were extracted from mouse cerebellum and hippocampus using the RNeasy kit (Qiagen) and retrotranscribed by the SuperScript II first-strand synthesis system (Invitrogen). We evaluated the relative *GRK4* mRNA expression in mouse cortex, hippocampus and cerebellum in adult wild-type versus *Fmr1* null mice by quantitative real-time polymerase chain reaction (PCR) by this set of primers: F: CCTGATCCTCAGGCCATTTATT, R: GGTATCCAGGTTGACTCCTTTCA. Real-time PCR was performed using LightCycler 480 Real-Time PCR System (Roche) using the cDNA, qPCR Core kit for SYBR Green (Eurogentec) according to the manufacturer's instructions and as previously described (6). All experiments were performed in triplicate. The relative expressions of transcripts were quantified using $2^{-\delta\delta CT}$ method. Mouse TBP gene was used as a housekeeping gene for normalization (15).

Western blot

Brain samples were thawed on ice, weighed and extracted in 2 ml/100 mg of cold extraction buffer (20 mM Tris pH 7.4, 2.5 mM MgCl2, 150 mM NaCl, 0.5% NP40) supplemented with antiprotease cocktail (Roche). Lysates were homogenized using a teflon potter fitted to 1.5 ml Eppendorf tubes and centrifuged at 10 000 *g* for 10 min at 4°C. Supernatant was collected, and protein content was determined by spectrometry at 580 nm using Bradford reagent (Biorad). A total of 25 μg of proteins were loaded on an 11% sodium dodecyl sulphate-polyacrylamide gel electrophoresis and western blotting was performed as previously described (16,17) using rabbit polyclonal anti-GRK4 (Sigma-Aldrich).

Plasmids and constructs

Human *GRK4* IMAGE clone 40125871 was used as a template to subclone the five fragments of GRK4 into pGEM-T easy vector (Promega) by PCR amplification using the appropriate primers whose sequences are reported in Table 1. Fragments S1/S2, S2/S3, DegS1/S2 and DegS3/S4 were generated using the primers listed in Table 2 and inserted in the 5′ UTR (StuI site), the 3′ UTR (PmeI site) or in frame in the middle of the coding sequence (EcorV site) of the Renilla luciferase (no stop codons have been generated) in the psiCHECK-2 vector (Promega). All constructs were verified by sequencing using a BigDye terminator sequencing kit and an ABI 3130XL sequencer (Applied Biosystems).

Production and purification of recombinant proteins

Escherichia coli BL21 star (DE3) cells (Invitrogen) were transformed with histidine-tagged pET151/D-Topo FMRP full-length, KH1, KH2 or RGG box constructs (6). The cells were grown in LB medium with ampicillin (100 mg/ml) and induced for 4 h at 20°C by addition of 1mM isopropyl-β-D-thiogalacto-pyranoside when the cultures reached an OD of 0.4 at 600 nm. Cells were then harvested and resuspended in lysis buffer [25 mM Tris–HCl pH 7.6, 300 mM KCl or LiCl, 1 mM EDTA, 1 mM dithiothreitol (DTT) , 20% glycerol, 5% NP-40, 0.5M urea, complete protease inhibitor cocktail (Roche), 1 mM PMSF] sonicated for 5 min and centrifuged at 15 000 r.p.m. for 30 min at 4°C. The supernatant was incubated with Ni-NTA Agarose beads (Qiagen) for 2 h at 4°C by agitation. Beads were washed four times at 4°C with washing buffer (25 mM Tris–HCl, pH 7.6, 300 mM KCl, 1 mM DTT, 0.5M urea, 20% glycerol, 20 mM imidazole). Fusion proteins were eluted from the beads with elution buffer (25 mM Tris–HCl pH 7.6, 50 mM KCl, 1 mM EDTA, 1 mM DTT, 10% glycerol, 0.1% Triton, 0.5M urea, 250 mM imidazole) for 30 min on ice.

RNA binding assays

RNA binding assay was performed as previously described (6,18–19) using a filter binding assay using Multiscreen Vacuum Manifold and the Multiscreen Separation System (Millipore). A total of 2 pmol of recombinant FMRP were used in each reaction.

CLIP (CrossLinking ImmunoPrecipitation)

Cerebellum fragments were sliced and dissociated in 6 ml cold PBS buffer and UV irradiated for 100 mJ/cm^2 in Stratalinker on ice. Lysis of cerebellum fragments was performed using the following lysis buffer: 50 mM Tris–HCl, pH 7.4; 100 mM NaCl; 1 mM $MgCl_2$; 0.1 mM $CaCl_2$; 1% NP-40; 0.5% sodium deoxycholate; 0.1% SDS; protease inhibitor (Roche) and ANTI-RNase (Life Technologies) added fresh. Partial RNA digestion was performed by adding 1 μl of a dilution (1/10 000) of RNase I (Ambion). FMRP/RNA complexes were immunopreciptated

Table 1. Primers used for cloning into pGEM-T easy

Fragments	Primers
GRK4–5′ UTR	F: CAGGGCACTGAGGAGGGAG R: GTCCTGGCGCCGCCGCC
GRK4-Cod1	F:ATGGAGCTCGAGAACATCGTG R: CAAACCTCTCCAAATCCGCC
GRK4-Cod2	F: GCGCCTGTCAAGTGCGAGC R:CTTGATTCTTTGATCGACCTCC
GRK4-Cod2a	F:GCGCCTGTCAAGTGCGAGC R: GTATACAATTCTTTCCCTCTG
GRK4-Cod2a-a	F:GCGCCTGTCAAGTGCGAGC R:CAAGCACAAGGCATCTTTGG
GRK4-Cod2a-b	F:CCAAAGATGCCTTGTGCTTG R:GTATACAATTCTTTCCCTCTG
GRK4-Cod2b	F:CAGAGGGAAAGAATTGTATAC R:CTTGATTCTTTGATCGACCTCC
GRK4-Cod3	F:AATGATACCGAGGAGTATTCTG R:GAAGTCTTCATCTGCGGTGTC
GRK4-Cod4	F:GACACCGCAGATGAAGACTTC R: CAGGTGGGACGAGACGCTAA

Table 2. Primers used for cloning into psiCHECK-2 vector

Fragments	Primers
S1/S2	F:TGCTTGGTGCTCACCATTATGAATGGAGGGGATTTGAAGTTTCACATTT R:GGCTCTCTGCTCATCAAAGCCGGGATTGCCCAGGTTGTAAATGTGAAA
DegS1/S2	F:TGCCTGGTGCTGACCATTATGAACGGCGGCGATCTGAAATTTCATATTT R:CGCGCGCTGTTCATCAAAGCCCGGGTTGCCCAGGTTATAAATATGAAAT
S3/S4	F:TTTGATGAGCAGAGAGCCGTTTTCTATGCTGCAGAGCTGTGTTGCGGC R: GTATACAATTCTTTCCCTCTGTAAATCTTCCAAGCCGCAACACAGCTCT
DegS3/S4	F: TTTGATGAACAGCGCGCGGTGTTTTATGCGGCGGAACTGTGCTGCGGC R:ATACACAATGCGTTCGCGCTGCAGATCTTCCAGGCCGCAGCACAGTTCC

overnight using protein A Dynabeads coupled to anti-FMRP R60 antibody (20). Beads were then washed using a high salt washing buffer: 50 mM Tris–HCl, pH 7.4; 1 M NaCl; 1 mM EDTA; 1% NP-40; 0.5% sodium deoxycholate; 0.1% SDS. FMRP was then degraded using 25 μg proteinase K and the RNA was extracted by phenol/chloroform. RNA fragments were precipitated then reverse transcribed using random hexamers. cDNA was used to perform real time PCR analysis using the primers described in Table 3.

G-quadruplex-forming structure detection

The presence of a G-quadruplex structure in the *GRK4* mRNA was tested both by reverse transcriptase-mediated primer extension following a protocol adapted from (18). Briefly, 100 ng of target RNA and 100 000 cpm of a 5′-end labeled primer were heat denatured for 1 min at 90°C, then oligo was allowed to anneal to the template RNA for 5 min at 20°C in HB-folding buffer (50 mM Hepes pH 7.0, 100 mM NaCl or KCl or LiCl, 167 nM EDTA). Primer extensions were initiated by the addition of RT elongation mix, containing 50 mM Tris ph8.5, 6 mM MgCl2, 40 mM NaCl or KCl or LiCl, 1 mM dNTP and 3 unit of Superscript II (Invitrogen). RT were performed at 37°C for 30 min, then cDNA was precipitated with ethanol. After centrifugation the pellet was resuspended in 6 μl of RNA loading buffer 2 (Ambion). cDNA was separated on 8% denaturing PAGE gel (National Diagnostic). Gels were then fixed in a solution of 10%EtOH-6%Acetic acid in water, and dried on an electrophoresis gel dryer (Biorad) and exposed over night on BAS-MP Fujifilm imaging plate (Fujifilm) or images were acquired with a FLA-5100 image reader (Fujifilm). The presence of G-quadruplex-forming structures was detected by elongating γ-^{32}ATP 5′-end labeled primers: R2 (5′ CTTGATTCTTTGATCGACCTCC') for the *GRK4* mRNA, R2A (5′ GTATACAATTCTTTCCCTCTG 3′) for the *Cod2* mRNA and *FMR1*_FBS _(5′ CTTTAGCCTCTCTTGGATTAC 3′) for the two control RNAs N19 (positive control) and Δ35 (negative control).

Table 3. Primers for qPCR for CLIP

GRK4 fragments	Primers for qPCR
GRK4–5′ UTR	F: TCCTCAAAGGACAAGGGATG R: TTTCCGACGTCGAACTTTTC
GRK4-Cod1	F: GAACTTCGTGGCCAACAATC R: CTGACTGGGGGAAACTTCAG
GRK4-Cod2	F: CAAGTACGAGCTACAGGAAAAATGT R: CTATGCAATTTTTCTAAGATTCTTTTT
GRK4-Cod3	F: AAGTCCCAGAAGGGGAGATG R: CCCCACCAGTCAGGACTAAA
GRK4-Cod4	F: AGGGAGCCAACAGAACACTG R: TGGAAAGGACAAGACACTGAG
Hprt	F: GTAATGATCAGTCAACGGGGAC R: CCAGCAAGCTTGCAACCTTAACCA
TBP	F: AGGCCAGACCCCACAACTC R: GGGTGGTGCCTGGCAA

Chemical and enzymatic probing of Cod2a-β region

Cod2a-β RNA (3 pmoles) was denatured at 90°C for 1 min, then immediately incubated on ice for 1 min and equilibrated in the appropriate native buffer (50 mM Hepes buffer pH 7.5 for dimethyl sulfide (DMS) or borate buffer pH 8 for N-Cyclohexyl-N′-(2-morpholinoethyl-carbodiimide (CMCT) , 5 mM Mg acetate, 50 mM KOH acetate, 2 mM β-mercaptoethanol) for 15 min at room temperature (RT). Chemical modifications were performed in 20 μl final volume using either 1 μl of DMS (undiluted or diluted 1/2 in ethanol) or 60 or 20 μg of CMCT, at 20°C for 5 and 10 min, respectively and in the presence of 2 μg of yeast total tRNA (Ambion). Enzymatic modifications were performed with V1 (0.1 U and 0.01 U), T1 (0.05 U and 0.1 U) and A (1 μg/ml and 0.1 μg/ml) nucleases (Promega) for 5 min at RT, followed by ethanol precipitation. After solubilization in the appropriate buffer, modified RNAs were reverse transcribed using the γ-^{32}ATP 5′-end labeled GRK4-Cod2a-β_R primer, sequencing reactions and gel analysis were carried out as previously described (18).

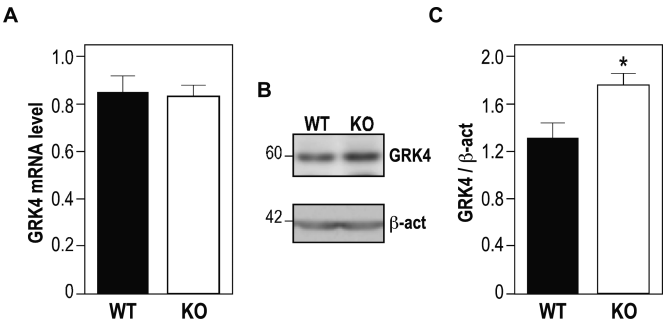

Figure 1. GRK4 expression in *Fmr1* null mouse cerebellum. (**A**) Quantitative RT-PCR reveals no difference between the *Grk4* mRNA level in cerebella obtained from 3 months aged wild-type mice (N=6) and from 3 months aged *Fmr1*-null mice (N=6). (**B**) Representative western-blot analysis of one cerebellum of wild-type mouse and one cerebellum of *Fmr1*-null mouse. Size of Grk4 (60 kD) and β-actin (42 kD) are indicated on the left of the western blot. (**C**) Densitometric analysis showing a significant increase of Grk4 expression: six cerebella of wild-type cerebella and six cerebella *Fmr1* knock-out mice are compared. Results are the average of Grk4 levels normalized by β-actin expression. Results are presented as the mean +/− SEM (Mann–Whitney test, $P < 0.05$).

Fluorescent primer extension of GRK4 mRNA

A modified *GRK4* mRNA harboring a sequence complementary to M13 Rev primer was generated by PCR using T7-grk-4 1110 F (gactgactTAATACGACTCACTATAGGGgactCCAAAGATGCCTTGTGCTTG) and m13_rev_grk4_1253_R (CACACAGGAAACAGCTATGACGTATACAATTCTTTCCCTCTG) primers. PCR product was purified (Qiagen Minelute Spin Column) and used as template in an *in vitro* transcription reaction incubated for 3 h at 37°C. The RNA product was purified by PAGE and its concentration was adjusted to 0.1 μg/μl. 5′-VIC®, 6-fluorescein amidite (6-FAM), NED® and PET® labeled M13rev primers (Life Technologies) were used at 1.25 μM. RNA structure was interrogated using various chemicals and enzymes, DMS, CMCT, RNAseT1, RNAseA and RNAseV1 as described above. The fluorescently labeled DNA primer were added to the modified T7–2a2_m13rev RNA (100 νg). VIC was used for the (+) and (−) reagent channels and NED or PET was used for the sequencing reaction channels. The RNA-primer solution was diluted to 6 μl with water and incubated at 95°C for 1 min, 4°C for 1 min and 20°C for 15 min in RT buffer (Tris–HCl 50 mM (pH 8,5), MgCl2 6 mM, KCl 40 mM). Primer extension was initiated by addition of enzyme mix [9 μl; Tris–HCl 50 mM (pH 8,5), MgCl2 6 mM, KCl 40 mM] and 2.5 mM dNTP and 20 units SuperScript II (Invitrogen). Reactions were performed at 37°C for 30 min. Sequencing reactions were identical, except that they used unmodified RNA (100 ng) and a modified dNTP set containing 1 mM of each dNTP, except the one corresponding to the dideoxy sequencing that was adjusted to 0.25 mM and 33 μM of this ddNTP. Extensions were quenched by precipitation with 100% ethanol,

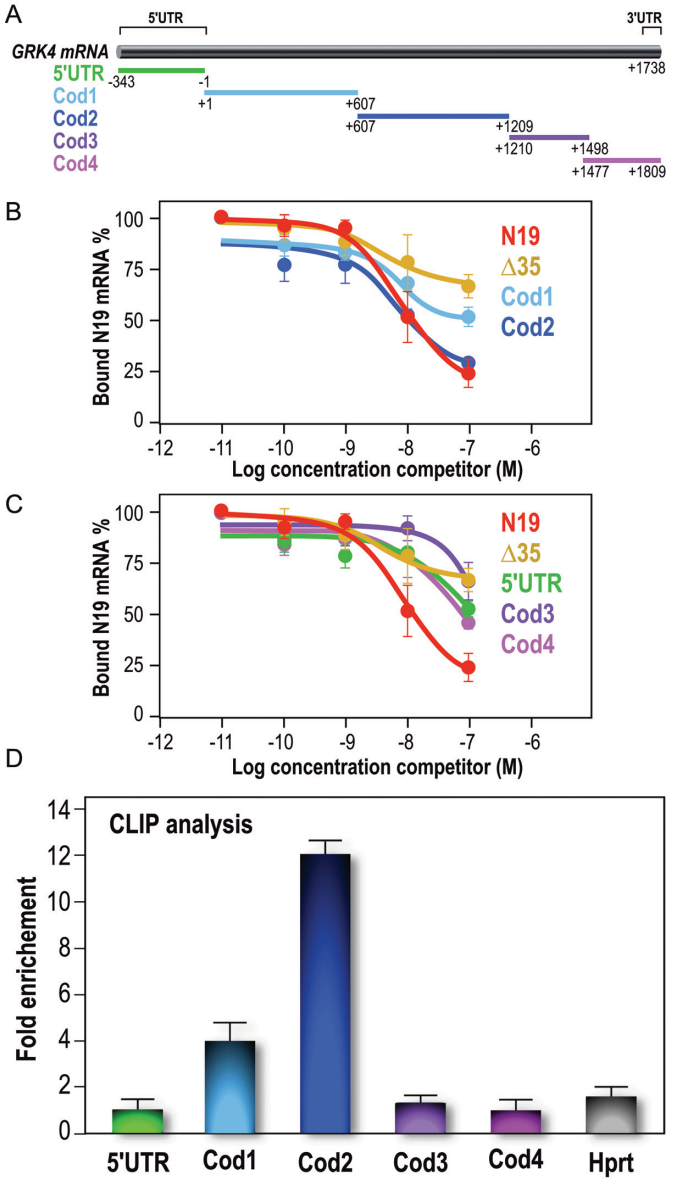

Figure 2. FMRP binds specifically *GRK4* mRNA *in vitro* and *in vivo*. (**A**) Schematic representation of human *GRK4* mRNA (BC117320) and the fragments subcloned from full-length cDNA and used to map the binding domain of FMRP on *GRK4* mRNA. (**B**) Binding specificity of FMRP to *GRK4* mRNA. Filter binding assay was performed by using full-length FMRP and ^{32}P-labeled N19 probe. The competition was performed using various regions of unlabeled *GRK4* mRNA: 5′ UTR region, Cod1, Cod2 fragments, N19 itself and Δ35 (the N19 fragment carrying the deletion of the G-quadruplex structure, as shown in Supplementary Figure S2A). The graph depicts the fraction of bound labeled N19 RNA plotted against unlabeled competitor RNA concentration. (**C**) The same experimental procedure described in (B) but the competition was performed using different regions of unlabeled *GRK4,* namely Cod3 and Cod4, and the two controls N19 and Δ 35. (**D**) CLIP analysis experiment. RNA co-immunoprecipitated with FMRP after UV-crosslink, was analyzed by qRT-PCR using specific oligos localized in the *GRK4* subdomains we determined for the *in vitro* analysis. *Hprt* was used as a negative control. Results are presented as the mean +/− SEM ($N = 4$).

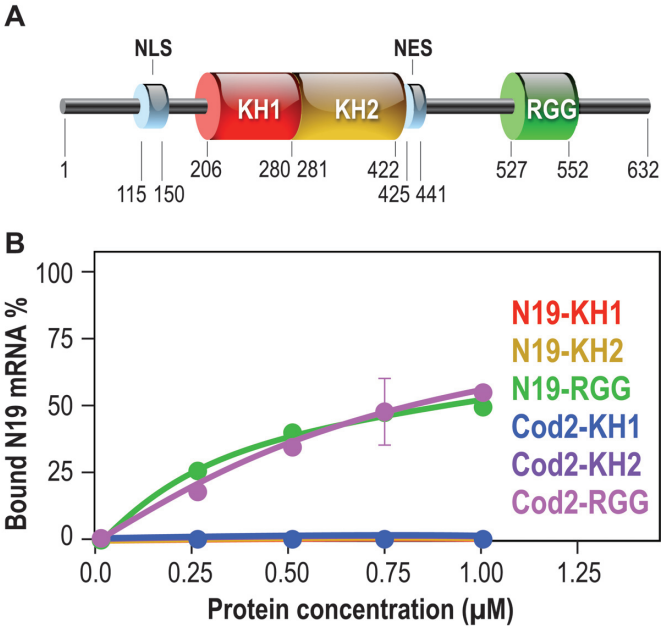

Figure 3. Domains of FMRP interacting with the mRNA of *GRK4*. (**A**) Architectural organization of FMRP domains. (**B**) Filter binding assay, using various recombinant RNA-binding domains of FMRP: KH1, KH2 and the C-terminal domain containing the RGG box and ^{32}P-labeled RNAs, reveals that the FMRP C-terminal domain (FCT) displays equal affinity for *Cod2* fragment or G-quadruplex (N19 RNA), whereas the two KH domains are not able to bind *Cod2* mRNA as well as N19 RNA.

washed with 70% ethanol and redissolved in 10 μl of highly deionized formamide supplemented with LIZ labeled DNA ladder (Life technologies), except the sequencing reactions that were resuspended in 5 μl of highly deionized formamide supplemented with LIZ labeled DNA ladder (Life technologies). Two sequencing reactions for each extension using the same primer sequence but labeled with a different fluorophore were mixed with one (+) or (−) reaction. Each resulting mix was loaded in a capillary on an Applied Biosystems 3130XL capillary electrophoresis DNA sequencer. Electropherograms were generated and analyzed with the QuShape software (21,22).

Luciferase assays

STEK cells, expressing or not FMRP (23) were seeded in 96-well plates (20 000 cells/well) and were immediately transfected with psiCHECK-2-derived constructs using Lipofectamine 2000 (Invitrogen) following the manufacturer's instructions with slight modification as follows: 60 ng of DNA were used per well with 0.5 μl of Lipofectamine 2000. After 48 h, medium was removed and cells were lysed in 70 μl of 1× passive lysis buffer (Promega); renilla and firefly activities were measured with the Dual-Glo luciferase assay system (Promega) using a Glomax 96-well plate luminometer (Promega). mRNA levels of Renilla and Firefly Luciferase were analyzed by RT-qPCR using the following primers:

- RLucF: TCCATGCTGAGAGTGTCGTG;
- RLucR: ATTTTCTCGCCCTCTTCGCT;
- FLucF: GACACCGCTATTCTGAGCGT;

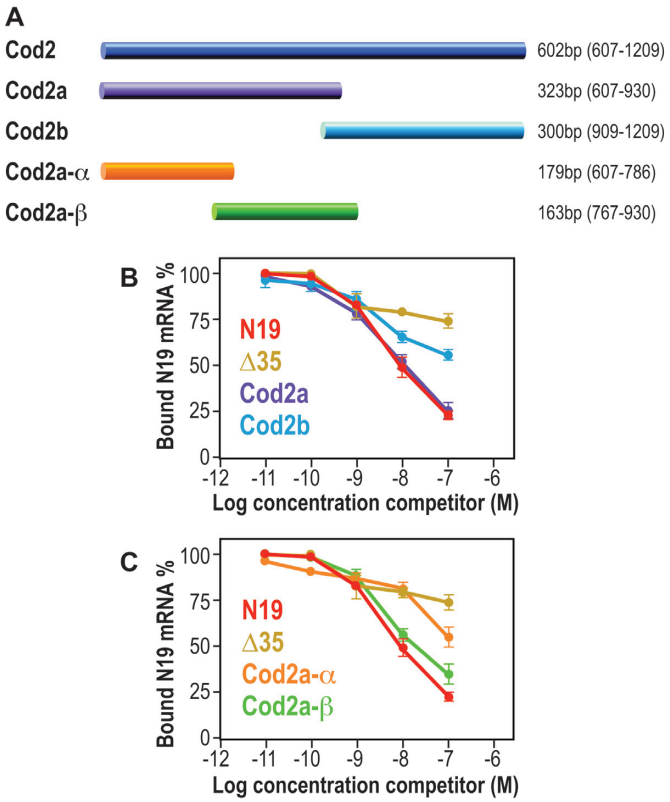

Figure 4. Sequences of the *GRK4* mRNA interacting with FMRP. (**A**) Scheme of the different subclones we generated from Cod2. Their size and their position in the coding sequence of GRK4 are indicated. (**B**) Filter binding assay using FMRP and ^{32}P-labeled N19. The competition was performed using various regions of unlabeled *GRK4* mRNA: Cod2a and Cod2b fragments. The two control N19 and Δ35 were also used as competitors. (**C**) Filter binding assay using FMRP and ^{32}P-labeled N19. The competition was performed using various regions of unlabeled *GRK4* mRNA: Cod2a-α and Cod2a-β fragments. The two control N19 and Δ35 were also used as competitors. Each experiment was repeated four times.

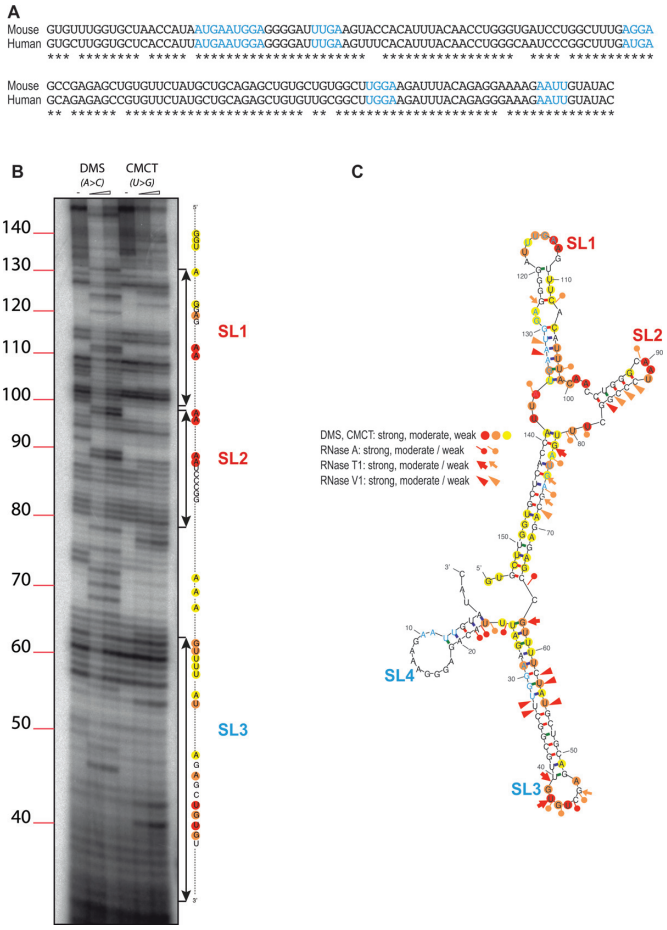

Figure 5. Sequence and structure of RNA domains interacting with FMRP. (**A**) Mouse and human sequence of G4RIF. The ACUK/WGGA motifs are highlighted in blue. (**B**) Six percent PAGE gel showing the running of retro transcribed G4RIF cDNA after treatment with DMS (modifying unpaired A and C) or CMCT (modifying unpaired G and U) (see also (6)). (**C**) RNA secondary structure model of G4RIF showing results from enzymatic cleavage and chemical modification experiments. The symbols indicating the reactivity are displayed and ACUK/WGGA sequences are shown in blue characters like in (A).

- FLucR: GTACATCAGCACCACCCGAA

Statistical analyses

All statistical analyses and graphs were realized using the GraphPad Prism Version 6.0e. http://www.graphpad.com/support/faq/whats-new-in-prism-mac-60e/.

RESULTS

Grk4 expression is impaired in the cerebellum of *Fmr1*-null mice

Grk4 mRNA has been found to be a component of FMRP-containing mRNP-complexes in cultured primary neurons by using the APRA (Antibody-positioned RNA amplification) technique (24). In order to assess whether FMRP modulates GRK4 expression, we studied *Grk4* levels in the presence or in the absence of FMRP in various brain regions. We tested the expression of *Grk4* mRNA in mouse cerebellum, hippocampus and cortex in wild-type versus *Fmr1* null adult animals. No differences have been observed in *Grk4* mRNA level by RT-qPCR in any analysis we performed in two different genetic backgrounds (C57BL/6 and FBV) (Figure 1A). Conversely, the expression of GRK4 protein by western blot in the cerebellum of wild-type and *Fmr1* adult knockout mice showed a higher level (30%) in both genetic backgrounds in the absence of FMRP (Figure 1 B and C), while no differences were observed in hippocampus and cortex of mice (not shown) at the same age. These results suggested that FMRP modulates the expression of GRK4 at the translational level acting as a repressor, as it has also been shown for many other mRNA targets of this protein (4).

FMRP binds the mRNA of GRK4 *in vitro* and *in vivo*

To show that *GRK4* mRNA is a target of FMRP, we decided to test FMRP/*GRK4* mRNA interaction *in vitro* and *in vivo*. To this purpose, we subcloned the cDNA of human *GRK4* into five fragments (Figure 2A) and we used these cDNAs to produce the corresponding RNAs and to test their interaction with FMRP by a filter binding assay in the pres-

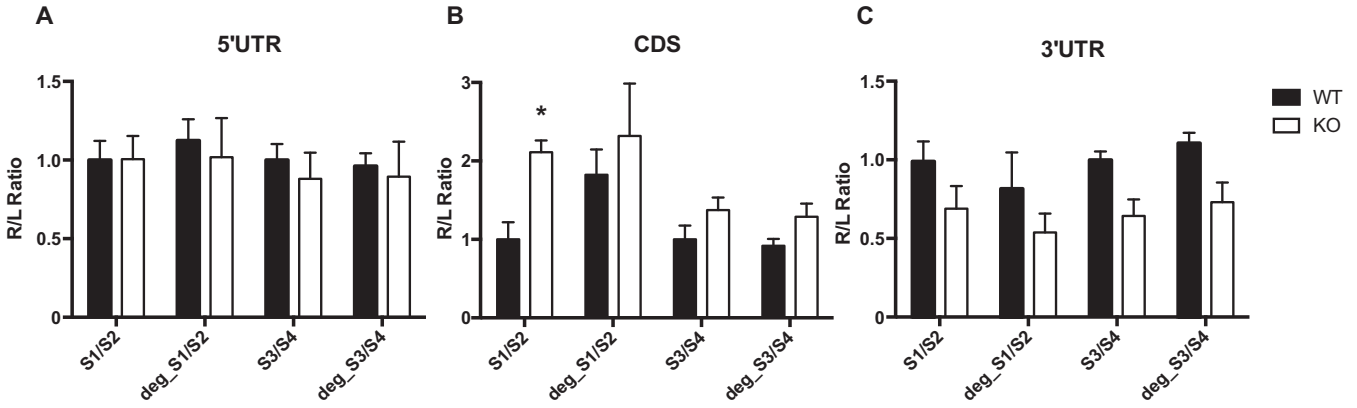

Figure 6. Influence of FMRP on luciferase reporter gene assay bearing G4RIF. psiCHECK-2 plasmid expressing Renilla bearing S1/S2 or S3/S4 or DegS1/S2 or DegS3/S4 G4RIF subregions were transfected in STEK cells. Three independent experiments with three replicates for each transfection, were quantified. For each transfection Renilla luciferase activity (R) was normalized with Firefly luciferase activity (L). In order to facilitate the comparison between native and degenerated sequences in WT and KO cells, ratios for all conditions were divided by the mean of the signal obtained for the cognate native sequences in the WT cells. Results are presented as the mean ±SEM (two way ANOVA, $*P < 0.05$). (**A**) S1/S2 or S3/S4 or DegS1/S2 or DegS3/S4 sequences have been cloned in the 5′ UTR of the Renilla reporter; (**B**) S1/S2 or S3/S4 or DegS1/S2 or DegS3/S4 sequences are cloned in frame with the coding sequence of the reporter gene; (**C**) S1/S2 or S3/S4 or DegS1/S2 or DegS3/S4 sequences are cloned in the 3′ UTR of the reporter gene.

ence of competitor RNA, the N19 probe contaning a G-quadruplex-forming structure, a motif that is well-known to interact with the RGG-box domain of FMRP (18,25). Only the Cod2 fragment competes with N19 mRNA binding to FMRP with the same affinity as N19 mRNA itself (Figure 2B). The *Cod1* mRNA competed with N19 binding to FMRP with very low affinity (Figure 2B) (one order of magnitude lower than *Cod2*) and, on the basis of our previous experience (18), we did not further study a target having such a weak affinity for FMRP. The other four fragments do not interact with FMRP since they did not compete with N19 binding to FMRP (Figure 2C), similarly to the negative control Δ35 (the N19 probe carrying a deletion of 35 nt that are key in the G-quadruplex folding structure) (26). To confirm FMRP/*GRK4* mRNA interaction *in vivo*, we used CrossLinking ImmunoPrecipitation (CLIP) analysis. After UV irradiation, cerebellum slices obtained from wild-type and *Fmr1* null mice were lysed and the extracts were subjected to mild RNAse digestion. Immunoprecipitation of FMRP mRNA complexes was carried out on these extracts using the polyclonal anti-FMRP antibody #R60 (20) (Supplementary Figure S1). RT-qPCR analysis of mRNAs extracted from both input RNAs and immunoprecipitates was then carried out using primers located in the five subregions of the mRNA of *GRK4* previously defined and using *Hprt* as a negative control. This analysis revealed an enriched association of FMRP with the *Cod2* region and a modest association with the *Cod1* region (Figure 2D), confirming the *in vitro* results we obtained (Figure 2B).

RGG-box domain is involved in *GRK4* mRNA/FMRP interaction

To assess which domain of FMRP was able to interact with *GRK4* mRNA, we produced the protein fragments of the different RNA-binding domains of FMRP (KH1, KH2, KH1/2 and RGG box-containing-C-terminal domains) as recombinant proteins in a bacterial system (6) and we used them in binding assays with the *GRK4-Cod2* RNA. The structural organization of FMRP is shown in Figure 3A. Interestingly, we observed that *GRK4-Cod2* RNA interacts only with the C-terminal domain of FMRP (RGG) (Figure 3B), similarly to the positive control, the N19 RNA. Conversely, *GRK4-Cod2* RNA was not able to interact with any of the KH domains even at high protein concentration (Figure 3B). The RGG box domain is known to bind not only to the G-quadruplex RNA structure (25) but also to the So-SLIP motif (6).

Definition of the critical region of *GRK4* RNA bound by FMRP

In order to define the molecular determinant of the FMRP/*GRK4* mRNA interaction, we decided to finely define the RNA fragment of *GRK4* that is bound by FMRP. For this purpose, we generated the sub-clones Cod2a and Cod2b from the Cod2 fragment (Figure 4A) and we performed a binding assay that allowed us to show that only the RNA obtained from the Cod2a fragment interacts with FMRP by competing the FMRP/N19 interaction with the same affinity as Cod2 (Figure 4B). We also generated two sub-clones from Cod2a, namely Cod2a-α and Cod2a-β (Figure 4A). Binding assay revealed that only the RNA obtained from the Cod2a-β mRNA interacts with FMRP by competing the FMRP/N19 interaction with the same affinity as Cod2/Cod2a (Figure 4C), while the Cod2-α RNA did not compete with the N19 probe. Since the *GRK4-Cod2a-β* RNA sequence harbors several ACUK/WGGA (27) motifs that are targeted by FMRP and that can fold in a G-quadruplex forming structure (11), we investigated the presence of a G-quadruplex in the *GRK4* mRNA critical region for FMRP interaction. We took advantage of the property of G-quadruplex forming regions to exhibit strong reverse transcription pauses when performed in K^+ containing buffer (18,23). Indeed, stabilization of G-quadruplex structures by K^+, but not by Li^+ or Na^+, results in cation-dependent pauses detectable on a sequencing gel that are readily observable when using for the positive control se-

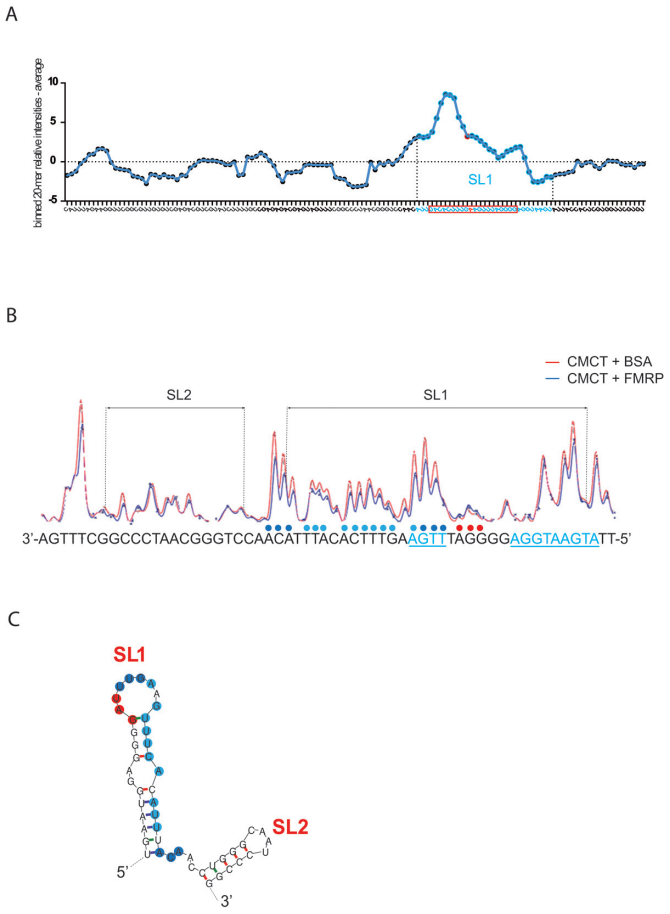

Figure 7. FMRP protection of SL1. (**A**) Relative CMCT reactivities along the G4RIF sequence. We used the QuShape software to quantify the reactivities of each nucleotide toward the CMCT probe in the presence of BSA or FMRP. BSA reactivities were subtracted to those in the presence of FMRP, providing a relative reactivity of each nucleotide to the CMCT probe in the presence of FMRP along the whole G4RIF sequence (Supplementary Table SI). We then summed the relative reactivities for 20 consecutive nucleosides to identify the sequence that is protected by FMRP. The relative reactivities of these 20-mer bins were plotted as a function of the G4RIF sequence. A sharp increase in the computed relative reactivities, highlighting the protection by FMRP, corresponds to the SL1 part of G4RIF sequence that is represented with blue dots on the graph. An exemple of a 20mer bin, centered on a ≪ A ≫ whose relative reactivity is shown as a red plot on the graph, is represented by the red rectangle at the bottom of the figure. (**B**) CMCT reactivities along the SL1 and SL2 part of the G4RIF in the presence of BSA (red line) or FMRP (blue line) are displayed with the corresponding sequence at the bottom of the figure. In the presence of FMRP (1 μM), a 20 nt sequence at the 3' end of SL1 is less reactive toward the CMCT probe than in the presence of BSA (1 μM). Colored dots above the sequence represent the relative protection by FMRP. Dark blue dots represent a stronger protection than light blue dots. Red dots represent a higher sensitivity to the CMCT probe in the presence of FMRP. ACUK/WGGA sequences are displayed in blue and underlined. (**C**) RNA secondary structure model of SL1/SL2 sequence showing results from chemical modification experiments in the presence of FMRP. Dark blue dots represent a stronger protection than light blue dots. Red dots represent a higher sensitivity to CMCT probe in the presence of FMRP.

quence N19 (Supplementary Figure S2A). The experiments were performed both on the *Cod2a* and *GRK4* mRNAs (as explained in 'Materials and Methods' section and in the legend of the Supplementary Figure S2) in order to completely cover the *Cod2* RNA fragment. This analysis allowed us to show that the fragments do not exhibit any pause in the presence of K^+, ruling out the presence of a G-quadruplex structure in the *Cod2* mRNA (Supplementary Figure S2B) as well as in the negative control Δ35 (Supplementary Figure S2A). These data were confirmed by *in silico* prediction using the QGRS web tool http://bioinformatics.ramapo.edu/QGRS/index.php (not shown).

Structure of G4RIF, the minimal region of the *GRK4* mRNA interacting with FMRP

The human and mouse sequences of *Cod2a*-β RNA are shown in Figure 5A. They display 81% identity and contain five ACUK/WGGA motifs, that are highlighted in blue in the figure. To unravel the molecular bases of *GRK4*/*FMRP* interaction we decided to determine the structure of the GRK4 Critical RNA Region Interacting with FMRP (G4RIF). To this purpose, we probed the structure of this region in solution, using a panel of chemical and enzymatic modifications (Figure 5B), as previously described (6). Our analysis showed a complex structure organized in two pairs of stem-loops that we named SL1, SL2, SL3 and SL4. SL1 loop harbors a ACUK/WGGA motif (UUGA), while other ACUK/WGGA motifs are localized in regions of double-stranded RNA (stem) (Figure 5C) (Supplementary Figures S3 and S4).

Role of the FMRP/G4RIF complex in translation

To investigate the functional role of the *G4RIF*/FMRP complex in translation we sub-fractioned Cod2a-β in two fragments S1/S2 encompassing SL1 and SL2 stem loops and S3/S4 encompassing SL3 and SL4 stem loops. The corresponding sequences were inserted in the 5′ UTR, in the 3′ UTR or in the coding sequence of the Renilla luciferase in the psiCHECK-2 vector. To control for the specificity of binding to FMRP, we subcloned also the degenerated S1/S2 and S3/S4 sequences (DegS1/S2 and DegS3/S4 constructs, respectively) at the same position as the native sequences in the 5′ UTR, in the 3′ UTR or in the coding sequence of the Renilla luciferase in the psiCHECK-2 vector. These mutated sequences give rise to the same protein sequences but fold into different RNA structures than the native S1/S2 and S3/S4 sequences, according to the mfold program (http://helix.nih.gov/apps/bioinfo/mfold.html). We transfected STEK fibroblasts expressing or not the *FMR1* gene (23) with the different constructions or with the psiCHECK-2 vector and we measured Firefly (F) and Renilla (R) luciferase activities. The ratio of the R on F activities showed on average two-fold increase ($P < 0.05$ two way ANOVA) when S1/S2 mRNA is in frame with the R luciferase coding sequence the (Figure 6B), but not for any of the other conditions (Figure 6A and C), suggesting the relevance of the S1/S2 domain in translational regulation via the G4RIF/FMRP interaction. We could also verify by RT-qPCR that the relative level of expression of the R luciferase mRNA of each construct were identical in the presence and in the absence of FMRP (not shown) when normalized by the F luciferase mRNA. Collectively, these findings confirm the data we obtained on en-

dogenous expression levels of Grk4 (mRNA and protein) shown in Figure 1.

To gain further insight into the mechanistic action of FMRP in translational regulation of GRK4, we also performed mapping experiments in the presence of FMRP. To precisely quantify the impact of FMRP on the G4RIF structure we used fluorescent primer extensions followed by capillary electrophoresis. We investigated the interaction of FMRP with the G4RIF using CMCT (that reacts with unpaired U and G nucleosides) and DMS (that reacts with unpaired A and C nucleosides) probes. We could map precisely FMRP interaction with the SL1/SL2 region of the G4RIF that is more reactive toward CMCT than DMS. Capillary electrophoresis signals obtained in the presence of bovine serum albumin (BSA) or FMRP were analyzed with the QuShape software (21,22). We calculated the relative reactivities of each nucleoside of the G4RIF in the presence of FMRP and in the presence of BSA (Supplementary Table SI). Since it was reported that the median protein footprint size is 40 nucleoside-long (28), roughly corresponding to the size of the S1/S2 fragment, we reasoned that to identify a consecutive stretch of protected nucleosides by FMRP, we could use a sliding window strategy using binned 20-mer in order to isolate the SL1 from the SL2 protections adapted from (29). To this purpose, for each nucleoside of the G4RIF, we summed the relative reactivities of the 10 preceding nucleosides and the 10 following nucleosides and plotted the result as a function of the G4RIF sequence (Figure 7A) and an example of our procedure is shown in Supplementary Table SI. This analysis highlighted clearly that the SL1 region is protected by FMRP (Figure 7A) from the CMCT probe. A close view at the electropherograms in the presence of FMRP or BSA (Figure 7B) confirmed that FMRP exerts a greater protection on the SL2 RNA from the CMCT probe than the BSA. We reported these protections on the G4RIF sequence (Figure 7C).

DISCUSSION

We describe here a new mRNA target of FMRP, the protein that is absent in FXS. This mRNA encodes GRK4, a member of the guanine nucleotide-binding protein (G protein)-coupled receptor kinase superfamily of the Ser/Thr protein kinase family. Our findings provide novel information concerning the role of FMRP in cerebellum and we propose that the absence of FMRP/*GRK4* mRNA interaction can have a role in the pathophysiology of FXS.

FMRP interacts with a new RNA motif: G4RIF

We identified the fragment (G4RIF) of the coding region of the *GRK4* mRNA that is bound specifically and with high affinity by FMRP and we defined its structure *in vitro*. Interestingly, this fragment is organized in four stem loops (namely SL1, SL2, SL3 and SL4) and contains five ACUK/WGGA sequences that have been described as short motifs mediating RNA/FMRP interaction (27). We noticed that many other ACUK/WGGA sequences are present in other mRNA regions of *GRK4* mRNA that do not interact with FMRP, leading to the conclusion that ACUK/WGGA motifs are not sufficient *per se* to mediate *GRK4* mRNA/FMRP interaction. In addition, we excluded that the WGGA motifs generate a G-quadruplex structure in the critical *G4RIF* mRNA, as predicted *in silico* for other mRNA targets of FMRP (11). Taken together, these results strongly suggest the existence of a new structure/motif mediating *GRK4* mRNA/FMRP interaction. Interestingly, a UUGA (ACUK/WGGA motif) sequence is present in the SL1 loop (Figure 5B), highly protected by FMRP (Figure 7C), and that is a part of the S1/S2 sequence that increases the translation of a reporter mRNA when inserted in frame with it. Since the G4RIF motif is part of the coding region of the *GRK4* mRNA, we suggest that the position of the UUGA in the stem loop is important in the context of the target mRNA in order to allow FMRP to carry out its function. As for *GRK4* mRNA, another study observed that most mRNAs are associated with FMRP on brain translating polyribosomes via their coding sequence (8), probably because FMRP also interacts with the ribosomal L5 protein blocking/stalling translation (30). Moreover, we also noticed that a ACUK/WGGA motif (AUGA) is located in loop 2 of the SoSLIP structure, a motif that we have shown to mediate FMRP/*Sod1* mRNA interaction (4,6). Collectively, these results suggest that the presence of ACUK/WGGA motifs can be relevant for FMRP function when located in a specific structural context. As in the two mentioned cases, we can speculate that the stem loop provides a structure that allows the UUGA or AUGA sequences to be accessible to FMRP binding. SoSLIP triggers translation activation while G4RIF is involved in translational repression, however SoSLIP is located at the end of the 5′ UTR/beginning of the coding sequence (being an IRES) (6), while G4RIF is located in the coding region of the *GRK4* mRNA (this study). Moreover, additional motifs or proteins can cooperate with FMRP to carry out its different roles in translation. Till date, studies of FMRP/RNA interaction generated two sets of results: (i) FMRP interacts with RNA structures such as G-quadruplex, SoSLIP, Kissing loop (4); (ii) FMRP recognizes short sequences such as ACUK/WGGA motif and polyU (4). Our findings suggest that both sequence and structure are important for FMRP interaction with RNA for some targets and they represent a valuable advance in the dissection of the molecular function of FMRP. To our best knowledge, this is the first study showing that FMRP specifically binds a motif resulting from a structure/sequence combination. Conversely, a sequence/structure combination is known to be bound by Smaug (31) and, in this case, the position of the targeted motif into the bound RNA does not appear to be relevant for its functional significance (32).

We observed that the RGG box domain mediates the interaction between FMRP and the *GRK4* mRNA. It is interesting to underline that another study reported that the FMRP KH2 domain interacts with the ACUK/WGGA sequences. This data was established considering that FMRP carrying the pathological, I304N mutation—causing a serious form of FXS—does not bind them (27). However, while we have shown a direct interaction between Cod2 RNA and the C-terminal domain of FMRP and no interaction with the KH1 and the KH2 domains, no isolated KH2 domain was tested in binding with ACUK/WGGA

sequences by the previous study (287). Thus, it might be possible that the I304N full length protein is not properly folded, resulting in a general loss of affinity for RNA and not only for ACUK/WGGA. Indeed, for instance, I304N was shown to be unable to interact with homopolymer poly (G) RNA (33), that is a non-specific target of FMRP In conclusion, the C-ter domain of FMRP binds ACUK/WGGA in a specific structural context (as for G4RIF and SoSLIP) or when these motifs are organized in G-quadruplex structures (4,11,18). We cannot exclude that KH2 may recognize and bind ACUK/WGGA sequences in a not yet identified structural motif other than G4RIF/SoSLIP or G-quadruplex. Remarkably, the *GRK4* mRNA represents an additional target RNA of FMRP bound by the C-terminal region of FMRP and likely by the RGG box domain. This aspect is very interesting and renovates the question of how this domain can bind and discriminate different RNA structures (e.g. G-quadruplex, SoSLIP, G4RIF) (4). Methylation is a modification that is important for FMRP RGG activity (34) and that could play a role in its capacity to bind mRNA (35). All our data were obtained using FMRP produced in bacteria, where such post-translational modification is not made. In addition, we confirmed our findings using recombinant FMRP produced in baculovirus and/or by *in vivo* CLIP analysis (6,18,23 and this study), thus excluding a role of a modified RGG box in its specificity of RNA binding.

Cerebellar dysfunction in FXS: possible pathophysiological role of altered expression of GRK4

An important aspect of our study is that we found an increased expression of GRK4 only in the cerebellum of *Fmr1*-KO mice compared with controls. This suggests that FMRP has an important role in this tissue to regulate the translation of this particular mRNA. GRK4 is a regulatory protein required to promote GBR desensitization. GBRs are metabotropic G-protein coupled receptors regulating multiple downstream signaling cascades (36). In particular, in cerebellum GBRs signaling has a relevant role in motor coordination and motor learning (13). It was reported that GRK4-dependent desensitization of GBR occurs in the absence of an increased receptor phosphorylation in cerebellum and does not require the catalytic activity of the kinase, suggesting that GRK4 possesses a function other than its kinase activity (12). Thus, in the absence of FMRP, an elevated level of GRK4 in cerebellum might promote a higher rate of constitutive desensitization of GBR specifically in this brain region contributing to deficits of motor learning and movement coordination that are cerebellum-dependent phenotypes of FXS patients (14). It is known that GBRs have a role also in the pathophysiology of FXS. Indeed an activation of GBRs by arbaclofen (a well known agonist of GBR) has been shown to correct some major phenotypes of the FXS mouse model (37) and improved behavior of a subgroup of FXS patients (38) but the effect of arbaclofen on motor learning/coordination was never monitored in detail. We propose here that molecules that can modulate the action of GRK4 might be useful to try specific therapies targeting cerebellum-dependent phenotype of FXS patients improving their quality of life.

A big effort has been performed during the last 15 years resulting in hundreds of mRNAs identified as targets of FMRP, however only a few motifs mediating these interactions have been precisely characterized. For these reasons, we are convinced that the full understanding of molecular bases of FMRP/RNA interaction is still far to be completed.

SUPPLEMENTARY DATA

Supplementary Data are available at NAR Online.

ACKNOWLEDGEMENT

The authors are grateful to Dr E. Lalli for critical reading of the manuscript, to Kevin Lebrigand for discussion, to Ricardo Tabet, Nathalie Leroudier and Frank Aguila for help.

FUNDING

INSERM; CNRS LIA NEOGENEX; Agence Nationale de la Recherche: ANR-11-LABX-0028-01, ANR-12-BSV4-0020, ANR-12-BSV8-0022-01; Equipe FRM DEQ20140329490; ARC (Fondation ARC pour la Recherche Sur le Cancer) Fellowship (to S.A.). Funding for open access charge: ANR-12-BSV8-0022-01 .
Conflict of interest statement. None declared.

REFERENCES

1. Bardoni,B., Davidovic,L., Bensaid,M. and Khandjian,E.W. (2003) The fragile X syndrome: exploring its molecular basis and seeking a treatment. *Expert. Rev. Mol. Med.*, **8**, 1–16.
2. Myrick,L.K., Hashimoto,H., Cheng,X. and Warren,S.T. (2015) Human FMRP contains an integral tandem Agenet (Tudor) and KH motif in the amino terminal domain. *Hum. Mol. Genet.*, **24**, 1733–1740.
3. Liu-Yesucevitz,L., Bassell,G.J., Gitler,A.D., Hart,A.C., Klann,E., Richter,J.D., Warren,S.T. and Wolozin,B. (2011) Local RNA translation at the synapse and in disease. *J. Neurosci.*, **31**: 16086–16093.
4. Maurin,T., Zongaro,S. and Bardoni,B. (2014) Fragile X Syndrome: from molecular pathology to therapy. *Neuro. Biobehav. Rev.*, **46**, 242–255.
5. Khandjian,E.W., Huot,M.E., Tremblay,S., Davidovic,L., Mazroui,R. and Bardoni,B. (2004) Biochemical evidence for the association of fragile X mental retardation protein with brain polyribosomal ribonucleoparticles. *Proc. Natl. Acad. Sci. U.S.A.*, **101**, 13357–13362.
6. Bechara,E.G., Didiot,M.C., Melko,M., Davidovic,L., Bensaid,M., Martin,P., Castets,M., Pognonec,P., Khandjian,E.W., Moin,H. *et al.* (2009) A Novel Function of Fragile X Mental Retardation Protein in translational activation. *PLoS Biol.*, **7**, e16.
7. Gross,C., Yao,X., Pong,D.L., Jeromin,A. and Bassell,G.J. (2011) Fragile X mental retardation protein regulates protein expression and mRNA translation of the potassium channel Kv4.2. *J. Neurosci.*, **31**, 5693–5698.
8. Darnell,J.C., Van Driesche,S.J., Zhang,C., Hung,K.Y., Mele,A., Fraser,C.E., Stone,E.F., Chen,C., Fak,J.J., Chi,S.W. *et al.* (2011) FMRP stalls ribosomal translocation on mRNAs linked to synaptic function and autism. *Cell*, **146**, 247–261.
9. Millevoi,S., Moine,H. and Vagner,S. (2012) G-quadruplexes in RNA biology. *Wiley Interdiscip. Rev. RNA*, **3**, 495–507.
10. Subramanian,M., Rage,F., Tabet,R., Flatter,E., Mandel,J.L. and Moine,H. (2011) G-quadruplex RNA structure as a signal for neurite mRNA targeting. *EMBO Rep.*, **12**, 697–704.
11. Suhl,J.A., Chopra,P., Anderson,B.R., Bassell,G.J. and Warren,S.T. (2014) Analysis of FMRP mRNA target datasets reveals highly associated mRNAs mediated by G-quadruplex structures formed via clustered WGGA sequences. *Hum. Mol. Genet.*, **23**, 5479–5491.

12. Perroy,J., Adam,L., Qanbar,R., Chenier,S. and Bouvier,M. (2003) Phosphorylation-independent desensitization of GABA(B) receptor by GRK4. *EMBO J.*, **22**, 3816–3824.
13. Stagg,C.J., Bachtiar,V. and Johansen-Berg,H. (2011) The role of GABA in human motor learning. *Curr. Biol.*, **21**, 480–484.
14. Huber,K.M. (2006) The Fragile X—cerebellum connection. *Trends Neurosci.*, **29**, 183–185.
15. Livak,K.J. and Schmittgen,T.D. (2001) Analysis of relative gene expression data using real-time quantitative PCR and the 2(-Delta Delta C(T)). *Methods*. **25**, 402–408.
16. Melko,M., Douguet,D., Bensaid,M., Zongaro,S., Verheggen,C., Gecz,J. and Bardoni,B. (2011) Functional characterization of the AFF (AF4/FMR2) family of RNA-binding proteins: insights into the molecular pathology of FRAXE intellectual disability. *Hum. Mol. Genet.*, **20**, 1873–1885.
17. Davidovic,L., Bechara,E.G., Gravel,M., Jaglin,X.H., Tremblay,S., Sik,A., Bardoni,B. and Khandjian,E.W. (2006) The nuclear microspherule protein 58 is a novel RNA-binding protein that interacts with fragile X mental retardation protein in polyribosomal mRNPs from neurons. *Hum. Mol. Genet.*, **15**, 1525–1538.
18. Schaeffer,C., Bardoni,B., Mandel,J.L., Ehresmann,B., Ehresmann,C. and Moine,H. (2001) The fragile X mental retardation protein binds specifically to its mRNA via a purine quartet motif. *EMBO J.*, **20**, 4803–4813.
19. Bechara,E., Davidovic,L., Melko,M., Bensaid,M., Tremblay,S., Grosgeorge,J., Khandjian,E.W., Lalli,E. and Bardoni,B. (2007) Fragile X related protein isoforms differentially modulate the affinity of fragile X mental retardation protein for G-quartet RNA structure. *Nuc Acids Res.*, **35**, 299–306.
20. Davidovic,L., Navratil,V., Bonaccorso,C.M., Catania,M.V., Bardoni,B. and Dumas,M.E. (2011) A metabolomic and systems biology perspective on the brain of the fragile X syndrome mouse model. *Genome Res.*, **21**, 2190–2202.
21. Deigan,K.E., Li,T.W., Mathews,D.H. and Weeks,K.M. (2009) Accurate SHAPE-directed RNA structure determination. *Proc. Natl. Acad. Sci. U.S.A.*,**106**, 97–102.
22. Karabiber,F., McGinning,J.L., Favorov,O.V. and Weeks,K.M. (2013) QuShape: Rapid, accurate, and best-practices quantification of nucleic acid probing information, resolved by capillary electrophoresis. *RNA*, **19**, 63–73.
23. Castets,M., Schaeffer,C., Bechara,E., Schenck,A., Khandjian,E.W., Luche,S., Moine,H., Rabilloud,T., Mandel,J.L. and Bardoni,B. (2005) FMRP interferes with the Rac1 pathway and controls actin cytoskeleton dynamics in murine fibroblasts. *Hum. Mol. Genet.*, **14**, 835–844.
24. Miyashiro,K.Y., Beckel-Mitchener,A., Purk,T.P., Becker,K.G., Barret,T., Liu,L., Carbonetto,S., Weiler,I.J., Greenough,W.T. and Eberwine,J. (2003) RNA cargoes associating with FMRP reveal deficits in cellular functioning in *Fmr1* null mice. *Neuron*, **37**, 417–431.
25. Darnell,J.C., Jensen,K.B., Jin,P., Brown,V., Warren,S.T. and Darnell,R.B. (2001) Fragile X mental retardation protein targets G-quartet mRNAs important for neuronal function. *Cell*, **107**, 489–499.
26. Bensaid,M., Melko,M., Bechara,E.G., Davidovic,L., Berretta,A., Catania,M.V., Gecz,J., Lalli,E. and Bardoni,B. (2009) FRAXE-associated mental retardation protein (FMR2) is an RNA-binding protein with high affinity for G-quartet RNA forming structure. *Nucleic Acids Res.*, **37**, 1269–1279.
27. Ascano,M. Jr, Mukherjee,N., Bandaru,P., Miller,J.B., Nusbaum,J.D., Corcoran,D.L., Langlois,C., Munschauer,M., Dewell,S., Hafner,M. *et al.* (2012) FMRP targets distinct mRNA sequence elements to regulate protein expression. *Nature*, **492**, 382–386.
28. Silverman,I.M., Li,F., Alexander,A., Goff,L., Trapnell,C., Rinn,J.L. and Gregory,B.D. (2014) RNase-mediated protein footprint sequencing reveals protein-binding sites thrughout the human transcriptome. *Genome Biol.*, **15**, R3.
29. Gilchrist,D.A., Fargo,D.C. and Adelman,K. (2009) Using ChiP-chip and ChIP-seq to study the regulation of gene expression: genome-wide localization studies reveal widespread regulation of transcription elongation. *Methods*, **48**, 398–408.
30. Chen,E., Sharma,M.R., Shi,X., Agrawal,R.K. and Joseph,S. (2014) Fragile X mental retardation protein regulates translation by binding directly to the ribosome. *Mol. Cell*, **54**, 407–417.
31. Crucs,S., Chatterjee,S. and Gavis,E.R. (2000) Overlapping but distinct RNA elements control repression and activation of nanos translation. *Mol. Cell*, **5**, 457–467.
32. Chen,L., Dumelie,J.G., Li,X., Cheng,M.H., Yang,Z., Laver,J.D., Siddiqui,N.U., Westwood,J.T., Morris,Q., Lipshitz,H.D. *et al.* (2014) Global Regulation of mRNA translation and stability in the early Drosophila embryo by the Smaug RNA-binding protein. *Genome Biol.*, **15**, R4.
33. Siomi,H., Choi,M., Siomi,M.C., Nussbaum,R.L. and Dreyfuss,G. (1994) Essential role for KH domains in RNA binding: impaired RNA binding by a mutation in the KH domain of FMR1 that causes fragile X syndrome. *Cell*, **77**, 33–39.
34. Thandapani,P., O'Connor,T.R., Bailey,T.L. and Richard,S. (2013) Defining the RGG/RG motif. *Mol. Cell*, **50**, 613–623.
35. Stetler,A., Winograd,C., Sayegh,J., Cheever,A., Patton,E., Zhang,X., Clarke,S. and Ceman,S. (2006) Identification and characterization of the methyl arginines in the fragile X mental retardation protein Fmrp. *Hum. Mol. Genet.*, **15**, 87–96.
36. Chalifoux,J.R. and Carter,A.G. (2011) GABAB receptor modulation of voltage-sensitive calcium channels in spines and dendrites. *Neurosci. J.*, **31**, 4221–4232.
37. Henderson,C., Wijetunge,L., Kinoshita,M.N., Shumway,M., Hammond,R.S., Postma,F.R., Brynczka,C., Rush,R., Thomas,A., Paylor,R. *et al.* (2012) Reversal of disease-related pathologies in the fragile X mouse model by selective activation of GABAB receptors with arbaclofen. *Sci. Transl. Med.*, **4**, ra128.
38. Lozano,R., Hare,E.B. and Hagerman,R.J. (2014) Modulation of the GABAergic pathway for the treatment of fragile X Syndrome. *Neuropsychiatr. Dis. Treat.*, **10**,1769–1779.